

Core excitons at the boron K edge in hexagonal BNB. M. Davies,* F. Bassani,[†] and F. C. Brown*University of Illinois at Urbana-Champaign, Urbana, Illinois 61801*

C. G. Olson

Ames Laboratory-US DOE, Iowa State University, Ames, Iowa 50011

(Received 23 January 1981)

High-resolution measurements of soft-x-ray absorption near the boron K threshold of hexagonal BN display a prominent peak at 192.0 eV. The angular dependence of this absorption for p -polarization geometry is consistent with a final state constructed mostly of π -like wave functions. Although higher-energy parts of the spectrum can be approximated by an effective-mass exciton theory, the 192.0-eV peak requires a substantial central-cell correction. This core exciton is thus highly localized in real space and delocalized in \vec{k} space. It seems likely that a mixture of σ - and π -like wave functions is necessary to describe the final state; this could account for the observed line strength at normal incidence which is not zero.

I. INTRODUCTION

Hexagonal BN is a layered crystal very similar to graphite, which has been extensively studied because it is strongly anisotropic and has a simple and highly symmetric crystal structure. Both crystals are composed of two-dimensional arrays of hexagons within which the bonding is largely covalent. The interaction between different layers is very weak, however, which results in much larger bond lengths between atoms in different layers than between atoms in the same layer. Unlike the stacking arrangement in graphite, the stacking in BN is such that hexagons are located one directly above another, with nearest-neighbor pairs always being one boron atom and one nitrogen atom. Graphite and BN are isoelectronic, but whereas graphite is a semimetal, hexagonal BN is an insulator with a band gap of approximately 4.3 eV,¹ roughly equal to the difference of the energies of the p states in boron and nitrogen. The existence of this band gap in such an anisotropic crystal provides opportunities for the comparison of calculated band structures with optical properties which can be measured at the valence-band threshold and also at inner-shell thresholds.

A prominent absorption peak at 192.0 eV can be resolved near the boron K threshold in high-resolution soft-x-ray absorption measurements using

either a synchrotron radiation source² or a conventional x-ray tube (bremsstrahlung) source.³ A similar feature has been observed in experiments on BF_3 and BCl_3 molecules in the gaseous state,^{4,5} for which the peak is ascribed to an "inner well" transition, denoted by $a'_1 \rightarrow a'_2$. The final state in this assignment strongly resembles a boron np_z excited atomic state and has a wave function oriented perpendicular to the plane of the molecule. In the gas phase, the molecules are randomly oriented, so that no anisotropy in the optical absorption will be observed. But in the case of the layered crystal BN, which has similar initial and final states of the boron atoms, anisotropic optical properties have been observed.²

The anisotropy observed in the features of the boron nitride spectra at the K threshold are related to the symmetry of the states near the conduction-band minimum. In a two-dimensional model of BN, the energy bands are classified as being either σ - or π -like, depending on the parity of their basis functions with respect to reflection in the layer plane. Band-structure calculations indicate that the conduction-band minimum is π -like, being constructed from p_z atomic orbitals.⁶ The early measurements of Brown *et al.*² revealed two peaks near the threshold, both of which had a dependence on the angle of incidence of x rays in the p -polarization geometry. However, the peak with lower energy

appeared to have less dependence on angle than the second. Because of this and the fact that the first peak did not reduce to zero intensity when the electric polarization vector \vec{E} was perpendicular to the crystal axis c , the first peak was not associated with a π -like final state. More recently, this assignment of σ symmetry to the first peak has been questioned on the basis of electron-energy-loss measurements which have selection rules similar to those of optical measurements and can display anisotropy.⁷

More detailed observations of the BN K threshold spectra utilizing synchrotron radiation are reported in this paper. Careful measurements of the x-ray absorption as a function of energy and angle in both the s -polarization and p -polarization geometries are described, and it is concluded that the peak at 192 eV is due to transitions to a core exciton state constructed mostly of π -like wave functions. In Sec. II, we identify the selection rules for these optical transitions in order to motivate the choice of experimental geometry. Details of the experiment are discussed and the experimental results are then displayed. Section III presents a modified effective-mass theory which enables us to fit the line shape of the observed spectra and to estimate the exciton binding energy. Section IV discusses the effects on core exciton states due to mixing of σ and π states away from critical points of the Brillouin zone. Section V summarizes and concludes the paper.

II. EXPERIMENTAL METHOD AND RESULTS

Transmission measurements were made using the Grasshopper monochromator⁸ Mark II at the Synchrotron Radiation Center, University of Wisconsin-Madison, Stoughton, Wisc. The monochromator was equipped with a 1200 lines/mm grating, providing a resolution of 0.065 Å (0.19 eV at 192 eV) at the 15- μ m slits used. All measurements were made on the 240-MeV storage ring Tantalus I.

Compression-annealed pyrolytic BN was cleaved, and thin basal plane sheets were mounted over beveled apertures ranging in size down to 350 μ m. Since the thinnest crystalline samples that could be easily prepared were quite opaque, pinholes and stray light were a potentially serious problem. Samples were glued completely around the edges to prevent light leaks between the sample and substrate as the angle of incidence changed. The absence of pinholes or other defects was assured by careful study with an optical microscope and also by confirming that angle-of-incidence data were consistent on both sides of normal incidence. Second-order radiation was of little importance because of the steep fall-off above 250 eV characteristic of Tantalus I. Baffles and a carbon filter were used to reduce stray light. The detector was a windowless secondary emission multiplier. A germanium photocathode enhanced the desired wavelength relative to the background. The limitations imposed by the remaining stray light will be pointed out in the discussion.

In order to study the optical anisotropy of a layered crystal such as BN, one makes absorption measurements as a function of angle with the crystal in one of two orientations, which are called the s -polarization geometry and the p -polarization geometry. These two geometries allow one to vary the orientation of the x-ray electric polarization vector with respect to the crystal axes. As illustrated in Fig. 1, the p -polarization geometry results in a variation of the angle between the electric vector \vec{E} and the crystal axis c as the sample holder is rotated. The optical path length (effective thickness) also increases as $\sec\theta$. For the s -polarization geometry the electric vector remains parallel to the layers of the crystal (perpendicular to the c axis), whereas the path length increases as $\sec\theta$ as in p -polarization. Measurements in the s -polarization geometry allow one to check the procedure used to normalize the data, which involves correcting for the increased path length. Then one may be confident that the same correction procedure, as applied to the p -

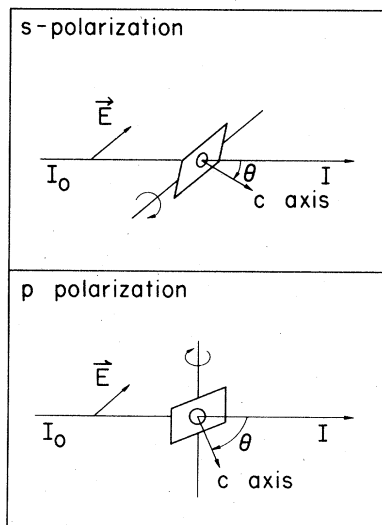


FIG 1. Sample orientation

polarization data, will allow the identification of true variation of the absorption coefficient as the angle θ is varied.

Properly normalized spectra for these two geometries are displayed in Figs. 2 and 3. The *s*-polarization curves, which have been displaced upward relative to each other for clarity, have very similar shapes. There are two angle-dependent effects of mechanical origin. Since the illumination overfills the sample aperture, there will be a decrease in transmission as the sample aperture decreases. This is a flat, additive baseline term in optical density. Secondly, the data must be scaled by $\cos\theta$ to correct the angle-dependent optical thickness. This has been done for Figs. 2 and 3. Measurements of samples with a range of thicknesses indicate that the relative magnitudes of the structures are not distorted by stray light and that the spectrum was not a strong function of the spread of microcrystalline structures in our samples. The monochromator resolution is high enough that the peak at 192 eV is not appreciably affected by instrument resolution.

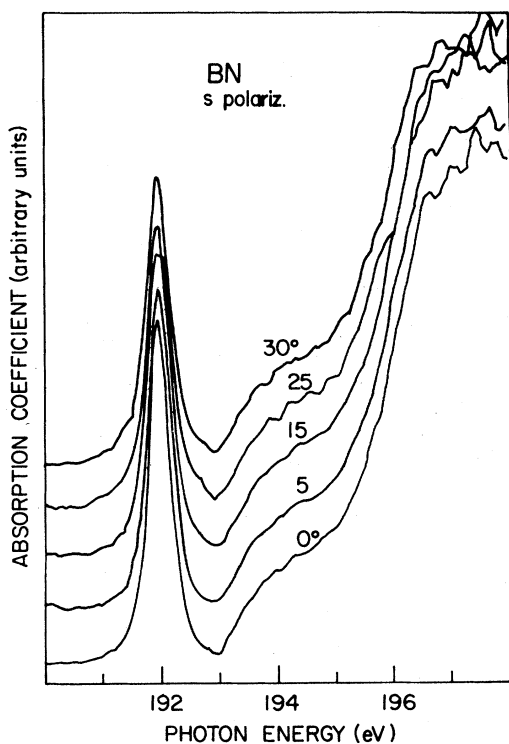


FIG 2. Absorption coefficient of BN in *s*-polarization geometry.

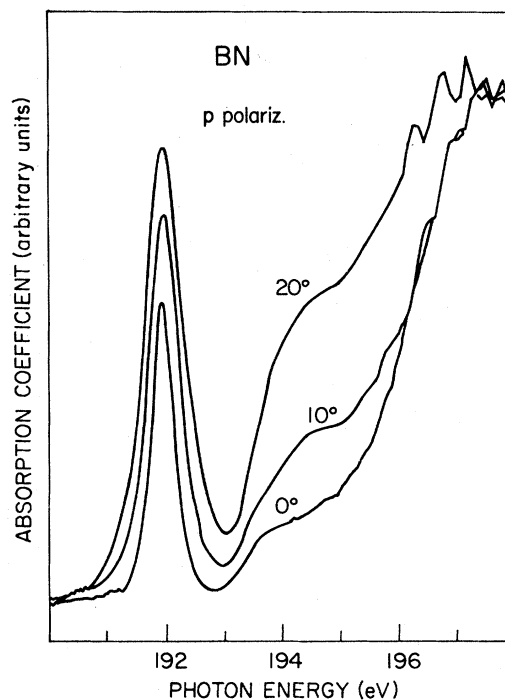


FIG 3. Absorption coefficient of BN in *p*-polarization geometry.

The *p*-polarization curves of Fig. 3 exhibit significant variation. As the angle θ increases and the component of \vec{E} along the *c* axis increases, the peak at 192 eV increases, as does the threshold structure extending from 193 to 196 eV. This angular dependence should help us identify the final states involved in these transitions.

Allowed optical transitions may be identified by using symmetry arguments. Tight-binding-band-structure calculations for two-dimensional BN indicate that the minimum of the conduction bands occurs at the symmetry point *P* (equivalent to the line *K-H* in the three-dimensional case).⁶ Assume that the observed transitions originate from boron 1*s* levels. Only the representation p_2^+ has the Bloch function s_B as a partner function. For incident radiation polarized parallel or perpendicular to the *z* axis of BN, the allowed transitions at point *P* are⁸

$$P_2^+ \rightarrow \begin{cases} P_2^- & \text{for } \vec{E} \parallel \hat{z} \\ P_1^+, P_3^+ & \text{for } \vec{E} \perp \hat{z} \end{cases} \quad (1)$$

The band structure diagram⁶ for two-dimensional BN indicates that the lowest conduction-band state

has symmetry P_2^- . Hence, optical transitions to the conduction-band minimum will occur only for incident electromagnetic radiation with a polarization vector which has a nonzero component along the z axis. The only partner function of the representation P_2^- is p_{zB} , hence the final-state wave function will be a p_z wave function centered on the boron atom.

As explained by Leapman and Silcox,⁷ in order to obtain the orientational dependence of optical absorption one may consider the dipole matrix element between atomiclike initial and final states (and not the Bloch states). The lowest conduction band is a so-called π band, which in two-dimensional BN is odd under reflection in the xy plane, and has Bloch states derived entirely from p_z wave functions. Taking the initial state as a boron $1s$ state and the final state as a boron $2p_z$ state, one finds that the transition matrix element $\langle 1s_B | \hat{e} \cdot \hat{r} | 2p_{zB} \rangle$ has an angular factor of $\sin(\pi/2 - \alpha)$, where α is the angle between the polarization vector \hat{e} and the crystal \hat{z} axis (i.e., $\hat{e} \cdot \hat{z} = \cos\alpha$). Similarly, the matrix element for transitions to states in a σ band has an angular dependence of $\cos(\pi/2 - \alpha)$. In the p -polarization geometry, defining $\theta = \pi/2 - \alpha$ as the angle between the crystal \hat{z} axis and the beam axis, the intensity should have an angular dependence proportional to the square of the matrix element, varying as $\sin^2\theta$ for π -like final states and $\cos^2\theta$ for σ -like final states.

Figure 3 shows that both the first (192 eV) and second features of the edge spectrum increase approximately as would be expected for features associated with states derived from π -like bands. Because the features do not reduce to zero, the experimental results for the s -polarization geometry (and

for $\theta = 0$ in the p -polarization geometry) are inconsistent with the interpretation that the final state is totally π -like.⁷ Possible mosaic spread or misalignment, assumed to be important in the previous work,² do not give large enough values of $\sin^2\theta$ to account for the strength of the $\theta = 0^\circ$ data relative to the $\theta = 10^\circ$ data shown in Fig. 3. The possible existence of an exciton final state constructed from a mixture of states with σ - and π -like symmetry is discussed in Sec. IV.

III. THEORY OF CORE EXCITONS IN THE EFFECTIVE-MASS APPROXIMATION

In this section the effective-mass approximation (EMA) will be applied to hexagonal BN in an attempt to explain the shape of the features near the K threshold. The EMA is generally applicable to materials in which the electron effective mass is small and which have large dielectric constants, so that the exciton envelope function is delocalized over many unit cells. Exciton states with principal quantum number $n > 1$ will generally satisfy this condition of delocalization. In the case of core excitons the electron may be delocalized even though the core hole is highly localized. Hence we expect the EMA to apply to higher ($n > 1$) exciton states and the unbound (continuum) states even in the case of BN. Corrections to the $n = 1$ state will be discussed later. Furthermore, matrix-element effects will not be considered, as we apply the EMA to $\theta = 0^\circ$ data.

The line shape for absorption near a fundamental edge, in the EMA with Lorentzian broadening, is given by Altarelli and Dexter⁹ as

$$\alpha(\hbar\omega) = |\langle \psi_f | \vec{p} | \psi_i \rangle|^2 \left[\frac{4\pi^2 e^2}{m^2 c \omega} \sum_n |F_n(0)|^2 \frac{\Gamma/2\pi}{(\hbar\omega - E_n)^2 + \frac{1}{4}\Gamma^2} + \frac{e^2}{m^2 c \omega} \left(\frac{2\mu}{\hbar} \right)^{3/2} \int_{E' > E_g} (E' - E_g)^{1/2} |F_{E'}(0)|^2 \frac{\Gamma/2\pi dE'}{(\hbar\omega - E')^2 + \frac{1}{4}\Gamma^2} \right], \quad (2)$$

where ψ_i is the initial (core) state, ψ_f is the Bloch function, and μ the effective mass at the bottom of the conduction band. Γ is the half-width of the Lorentzian, $\hbar\omega$ is the photon energy, and $|F(0)|^2$ is the absolute square of the exciton envelope function at the origin, so

$$|F_n(0)|^2 = \frac{1}{\pi n^3} \left(\frac{2\mu\mathcal{R}}{\hbar^2} \right)^{3/2} \quad (3)$$

for discrete states, and

$$|F_{E'}(0)|^2 = \frac{\pi\gamma e^{\pi\gamma}}{\sinh(\pi\gamma)} \quad (4)$$

for the continuum states, where $\gamma = [\mathcal{R}/(E' - E_g)]^{1/2}$. E_g is the energy of the absorption threshold, which can be estimated as the difference between the energies of the bottom of the conduction band and of the inner-shell band, and

E_n is the energy of the bound exciton state with principal quantum number n , given by $E_n = E_g - \mathcal{R}/n^2$ in the EMA, where the effective Rydberg is $\mathcal{R} = \mu e^4 / (2\hbar^2 \epsilon_0^2)$.

Estimates of \mathcal{R} and E_g may be derived from experimental results. Using infrared reflectivity and absorption techniques, Geick *et al.*¹⁰ have determined the static dielectric constant of BN and reports that $\epsilon_{\parallel} = 5.09$ and $\epsilon_{\perp} = 7.04$. We will replace these by an effective mean dielectric constant $\epsilon_0 = (\epsilon_{\perp} \epsilon_{\parallel})^{1/2} = 5.9$. Because we are unaware of any experimental measurements of the electron effective mass, we estimate μ using energy band calculations. The core-hole effective mass will be very large, so μ is approximately equal to the conduction-electron effective mass. Doni and Pastori Parravicini⁶ present two- and three-dimensional band-structure diagrams for BN. By approximating the band along $P \rightarrow Q$ as a cosine, we can obtain an estimate of $m_{\perp}^* = 2.3m$. The three-dimensional band diagram has a conduction-band minimum at H , and from it we estimate $m_{\parallel}^* = 1.9m$. From these estimates μ can be calculated using the relation¹¹

$$\frac{1}{\mu} = \frac{1}{3} \left[\frac{1}{m_{\parallel}^*} + \frac{2}{m_{\perp}^*} \right]. \quad (5)$$

The average isotropic effective mass is $\mu \simeq 2.2m$. The resulting effective Rydberg is

$$\mathcal{R} = \frac{\mu}{m} \frac{1}{\epsilon_0^2} (13.6 \text{ eV}) \simeq 0.8 \text{ eV}. \quad (6)$$

An experimental value of E_g may be obtained by adding the band gap, reported by Zupan and Kolar¹ to be 4.3 eV, to the energy difference between the B 1s level and the top of the valence band, which was measured by Tegeler *et al.*¹² using x-ray emission techniques as being 188.1 ± 0.5 eV. The sum is

$$E_g = 192.4 \pm 0.6 \text{ eV}. \quad (7)$$

When these values of \mathcal{R} and E_g are used in the Altarelli-Dexter equation (2), we do not get complete agreement with the experimentally observed energy of the first exciton peak, which is approximately 192.0 eV, as compared to the predicted value $E_g - \mathcal{R} = 191.6 \pm 0.6$ eV.

We investigated two possible modifications of the effective-mass theory which might result in a better estimate of the binding energy. One is the effect of anisotropy on the energy eigenvalues of the effective-mass equation. Gerlach and Pollman¹³ have displayed the binding energies of excitons as a function of an anisotropy parameter

$$A = \frac{\epsilon_{\perp} m_{\perp}^*}{\epsilon_{\parallel} m_{\parallel}^*}. \quad (8)$$

In the case of BN, we estimate $A \simeq 1.7$, but this is subject to large uncertainty because of our rough estimates for the effective masses. However, this value of A is substantially greater than the values required to significantly increase the binding energy. One must have $A < 0.3$ to get an increase of the binding energy of the $n = 1$ exciton by a factor of 1.5, and $A < 0.1$ to get a factor of 2. We conclude that anisotropy will not result in a large binding energy.

Another possible modification of the EMA is to include the effect of spatial dependence of the dielectric function. Quatropani *et al.*¹⁴ have shown that including the effects of a dispersive dielectric function results in substantially larger binding energies for the core excitations in Si. The binding energy is the lowest energy eigenvalue of the Schrödinger equation for the exciton envelope function. In a dielectric, the potential term must be modified from a simple Coulomb potential to the more general form:

$$V(r) = \frac{e^2}{\epsilon(r)r}. \quad (9)$$

Resta¹⁵ has applied a Thomas-Fermi model to semiconductors to obtain a simple expression for the dielectric function,

$$\epsilon(r) = \begin{cases} \frac{\epsilon_0 q r_0}{\sinh[q(r_0 - r)]}, & r \leq r_0 \\ \epsilon_0, & r > r_0 \end{cases} \quad (10)$$

where ϵ_0 is the static dielectric constant, $q = (4k_F/\pi)^{1/2}$ with k_F being the valence Fermi momentum, and r_0 is the positive solution of

$$\frac{\sinh(qr_0)}{qr_0} = \epsilon_0. \quad (11)$$

For BN, we use $\epsilon_0 = 5.9$, $q = 1.27$ a.u., and $\mathcal{R} \simeq 3$ a.u. or $\mathcal{R} \simeq 1.6$ Å. The radial Schrödinger equation with potential term $V(r)$ may be rewritten using substitutions analogous to those of Rogers *et al.*¹⁶ and the energy eigenvalues obtained in the manner discussed by French and Taylor.¹⁷ The binding energies are $1.9\mathcal{R}$ for the ground ($n = 1$) state and $0.33\mathcal{R}$ for the $n = 2$ state, as compared to the values \mathcal{R} and $1.25\mathcal{R}$ for the hydrogenic case $\epsilon(r) = \epsilon_0$. The higher ($n > 2$) states have binding energies close to \mathcal{R}/n^2 .

This so-called "central-cell correction" has result-

ed in an increase in the $n = 1$ binding energy by factor of 1.9 without substantially changing the other features of the absorption line shape. In Fig. 4 we display the Altarelli-Dexter line shape, using the following values: $E_1 = E_g - 1.9\mathcal{R}$, $E_2 = E_g - 0.33\mathcal{R}$, $E_n = E_g - \mathcal{R}/n^2$ for $3 \leq n \leq 20$, where $\mathcal{R} = 1.0$ eV, $\Gamma = 0.42$ eV, and $E_g = 193.9$ eV. The sum is taken up to $n = 20$ and the integral over $E_g < E' < E_g + 10$. This value of E_g is somewhat above the experimentally derived value mentioned above, and the value of \mathcal{R} which gives a good fit is close to the rough estimate of 0.8 given above. The relative amplitudes of the $n = 1$ exciton peak and the merged higher bound states and continuum in the region 193 to 195 eV are surprisingly well fitted by this calculation.

The relatively large central-cell correction required to fit the $n = 1$ exciton line indicates that the effective-mass approximation is perhaps inappropriate. At least the $n = 1$ state is localized in real space and relatively delocalized in \vec{k} space. It seems likely that a mixture of states is necessary to properly describe the core exciton in BN. This will be discussed in the next section. Ultimately, a detailed theory of the final state including the effect of the surrounding ligands (inner and outer well regions) is called for.

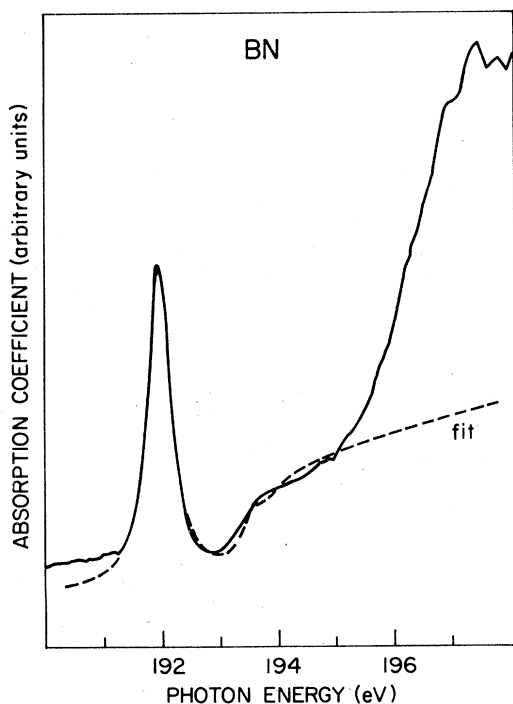


FIG 4. Altarelli-Dexter fit to BN spectrum.

IV. EFFECTS ON CORE EXCITONS DUE TO σ - π MIXING

The presence of "core exciton" features at $\theta = 0$ indicates that the simple symmetry arguments given in Sec. II fail to describe the final state as it depends upon the band structure of BN. Two methods have been used to calculate the band structure of the hexagonal BN: the tight-binding and the orthogonalized plane wave (OPW) methods.

In the first approach the band structure is obtained by considering the two-dimensional layer of hexagons, with alternating B and N atoms at the vertices, and combining the atomiclike s and p functions of both atoms to form the bonding states and the empty antibonding states. All valence and conduction bands can be classified by the angular momentum of their atomic functions and by their symmetry under the reflection σ_h in the xy plane. We then have s and p bands, and the p bands are subdivided into σ bands (even under σ_h) (p_x, p_y) and π bands (odd under σ_h) (p_z). In addition, an interaction between the p_z functions on different layers is considered, to account for a k_z dependence of the π bands. The results obtained with this procedure give small quantitative differences depending on the way in which the parameters of the tight-binding calculation (crystal fields and two-center integrals) are determined, but they basically agree with the general band structure, given by Doni and Pastori Parravicini.⁶

Doni and Pastori Parravicini,⁶ Zupan,¹⁸ and Zunger *et al.*¹⁹ all obtain well-separated σ and π bands and relatively small bandwidths. The highest valence band and the lowest conduction band are the bonding and antibonding π_z bands. The extrema are P_1^- and P_2^- at the point $\vec{k} = (2\pi/a)(\frac{2}{3}, 0, 0)$ of the basal plane of the Brillouin zone (BZ) in the two-dimensional limit and move to the edge of the BZ at $\vec{k} = 2\pi(2/3a, 0, 1/2c)$ when interaction between the p_z functions of different layers is taken into account.

In the second approach, developed by Nakhmanson and Smirnov,²⁰ one expands valence and conduction bands in plane waves, imposes orthogonality to the core levels, and diagonalizes the Hamiltonian with the crystal potential constructed as the sum of atomic potentials. In this case the connection with the atomic states is completely ignored, but can be recovered at the end by considering the sequence of the electronic levels at the symmetry points, and relating them to σ or π states according to their symmetry.

The results obtained with this approach are somewhat different from the tight-binding results. The bands are all much wider and less separated. In particular, the conduction bands σ and π are very close to the minimum of the conduction band; the minimum does not occur at the point H (corner of the Brillouin zone), but rather at the point L (midpoint at the edge of the BZ). This implies a strong admixture of σ bands and π bands at the points of the BZ along a line between $k_z = 0$ and $k_z = \pi/c$. The distinction between σ bands and π bands remains valid only on the basal planes; the admixture between σ and π functions should be considered at all other points of the zone.

It is difficult to obtain a detailed experimental picture of the band structure, other than the band gap and the general bandwidths. However, a recent analysis of the x-ray emission spectra of B and N indicates that the results of the OPW band calculations are in much better agreement with experiment.¹² If this is true for the valence band, we expect it to be even more appropriate for the conduction band, because it is well known that to reproduce the conduction band with the tight-binding method one should include additional localized functions in the expansion. The σ -like antibonding states are therefore expected to have consistently lower energies than those obtained from the tight-binding approximation and to mix with the π -like states.

It may then be safe to assume that a considerable σ - π mixing occurs at k_z away from the basal planes, an effect which was neglected in all previous calculations. We may estimate the admixture of σ and π wave functions near the minimum of the conduction band by considering the overlap and energy integrals (p_{z1}, p_{y2}) and (p_{z1}, p_{x2}) on the nearest B atoms of contiguous layers. The usual transformation formula expresses this in terms of $(pp\sigma)$ and $(pp\pi)$ integrals and the direction cosines of the distance d_{12} , and we can neglect the term $(pp\pi)$ in comparison with the larger term $(pp\sigma)$.

We must sum such contributions due to the six nearest atoms on both planes, which are obtained by considering the Bloch functions formed with p_{zB_1} , orbitals and with p_{yB_2} and p_{xB_2} orbitals. Along the direction $K-H$ of the Brillouin zone,

$$\vec{k} = \left[\frac{2\pi}{a} \frac{2}{3}, 0, \gamma \frac{\pi}{c} \right]$$

we have

$$\begin{aligned} (p_{zB_1}, p_{yB_2}) &= i(pp\sigma) \frac{ac}{d^2} \frac{\sqrt{3}}{2} \sin \left[\frac{\gamma\pi}{2} \right], \\ (p_{zB_1}, p_{xB_2}) &= (pp\sigma) \frac{ac}{d^2} \frac{\sqrt{3}}{2} \sin \left[\frac{\gamma\pi}{2} \right]. \end{aligned} \quad (12)$$

The appropriate combinations of Bloch functions which transform as the same row of the irreducible representation K_3 of the small group of the \vec{k} vector are p_{zB_1} and $p_{yB_2} + ip_{xB_2}$. From this we can obtain the admixture of σ and π functions on the B atoms. When this is taken into account the minimum of the conduction band may well occur away from the basal planes in the direction $K-H$ of the Brillouin zone.

Our results indicate that the minimum of the conduction band is indeed at $p_z \neq 0$, because the exciton absorption does not vanish for the component of the electric field in the basal plane, indicating a substantial σ - π mixing.

Let us suppose in fact that the equivalent minima of the conduction band are at $k_{z,c} \neq 0$ along the direction $K-H$. Since we are away from the basal planes the Bloch functions near the minima will be formed from a combination of π functions of boron atom B_1 and σ functions of boron atom B_2 ,

$$Z(k)p_{zB_2} + X(k) \left[\frac{p_y + ip_x}{\sqrt{2}} \right]_{B_2}, \quad (13)$$

and analogously from a combination of π functions of B_2 and σ functions of B_1 ,

$$Z(k)p_{zB_2} + X(k) \left[\frac{p_y - ip_x}{\sqrt{2}} \right]_{B_1}. \quad (14)$$

The above two functions will be degenerate in the direction $K-H$ because they belong to the same irreducible representation, but away from this direction will be split by π - π interlayer interaction, as shown by Doni and Pastori Parravicini.⁶

In the effective-mass approximation, which is certainly valid for $n > 1$ excitons, the exciton wave function is formed with the product of the hole function at $\vec{k}_{z,c}$ and of the electron function also at $\vec{k}_{z,c}$, when we neglect the small momentum of the photon, and therefore it contains a σ component and a π component. This is not in contradiction with the general requirement that the total many-electron Hamiltonian commutes with reflection on the basal plane σ_h , because the existence of a minimum at $k_{z,c} \neq 0$ implies an equivalent minimum at $-k_{z,c}$, and therefore every s -exciton state is degenerate in two states, one even and one

odd under σ_h .

For the exciton $n = 1$ the effective mass approximation is not strictly valid, and the two degenerate states of opposite parity under σ_h split by intervalley interaction. The magnitude of this splitting is not known and some disagreement exists among theorists who have tried to estimate it in Si.²¹ The fact that we obtain binding energy not too far from experiment also for $n = 1$ with the effective-mass approximation indicates that intervalley splitting is not larger than effective-mass binding energy and therefore the two states which are even and odd under σ_h are not resolved in the experiment. We can therefore have σ - π mixing in the exciton because of near degeneracy also in this case. The localization of the wave function in real space implies, however, that one cannot construct the exciton wave function for $n = 1$ only with Bloch functions at $k_{k,c}$, but one must expand on a region of \vec{k} space and also consider the contribution from higher conduction bands. We will have, in general, instead of the expansion coefficients $A_{ns}(k)$, which are the Fourier transforms of $F_{ns}(r)$, expansion coefficients $A_{1,m}(\vec{k})$ on functions (13) and (14), where m denotes the band index. This contains the effect of intervalley interaction, and if the even and odd states which result from this interaction are not resolved experimentally, the coefficients $A(k)$ may be taken to include both states, without a particular parity on k_z .

The polarization dependence of the transition probability, therefore, is more complicated than in the case of simple π bands. The oscillator strength for an s exciton with $n > 1$ is

$$\begin{aligned} & |F_{ns}(0)|^2 \left| \langle Z | s | \hat{e} \cdot \hat{r} | p_z \rangle \right. \\ & \left. + X \left\langle s \left| \hat{e} \cdot \hat{r} \left| \frac{p_y + ip_x}{\sqrt{2}} \right. \right. \right|^2. \end{aligned} \quad (15)$$

The oscillator strength for the lowest exciton ($n = 1$) is somewhat more complicated because the matrix element between core state $1s_B$ and the conduction band cannot be taken as the value at the extremum. One rather obtains for the oscillator strength, indicating with the index m the different conduction bands which may contribute,

$$\begin{aligned} & \left| \sum_{n,k} A_n(k) \langle Z_n(k) p_{zB} | \hat{e} \cdot \hat{r} | s_B \rangle \right. \\ & + \sum_{n,k} A_n(k) \langle X_n(k) p_{xB} | \hat{e} \cdot \hat{r} | s_B \rangle \\ & \left. + \sum_{n,k} A_n(k) \langle Y_n(k) p_{yB} | \hat{e} \cdot \hat{r} | s_B \rangle \right|^2, \end{aligned} \quad (16)$$

where the first term is polarized parallel to the c axis and the other two terms are polarized perpendicular to the c axis. The relative magnitude of the terms reflects both the σ - π admixture in the lowest conduction band due to interaction between different layers, and the contribution of higher conduction bands in the expansion of the wave function. The latter contribution may be considerable in the $n = 1$ exciton if the conduction-band-structure scheme of Nakhmanson and Smirnov²⁰ is correct.

Detailed theoretical calculations of the oscillator strengths cannot be made at present with sufficient reliability, because the general knowledge of the conduction band is not sufficiently accurate. However, one can estimate the σ - π mixing at the bottom of the conduction band and the average contribution of different bands from comparison with the experimental line shape and intensity at different polarization angles with respect to the c axis. The observed $n = 1$ exciton peak height has been truncated at higher angles due to stray light conditions mentioned in Sec. II, so that one must make corrections in order to find an experimental value for the oscillator strength of this feature. This correction consists of fitting a Lorentzian curve (of full width at half maximum = 0.5 eV) to those portions of the 10°

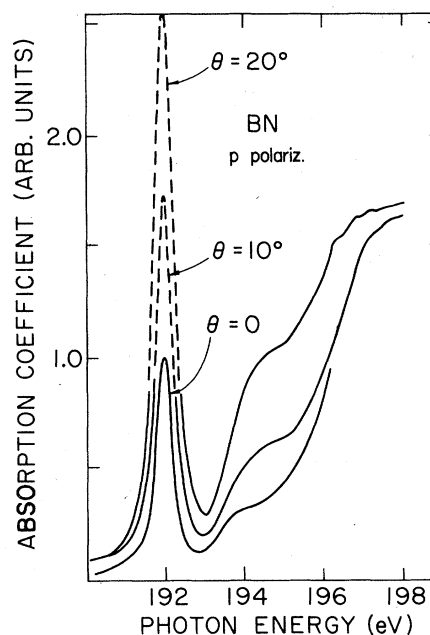


FIG. 5. Dashed lines show Lorentzian extrapolation of peak in p -polarization spectra. Solid lines are measured portions of spectra.

and 20° peaks which are below the peak of the 0° curve. This is based on the assumption that the width of the true peaks are the same, and that the 0° curve is undistorted as determined by measuring samples with a range of thicknesses. The extrapolated peaks are shown as dashed lines in Fig. 5, and have intensities in the ratio $1:1.8 \pm 0.1:2.6 \pm 0.2$ for the 0°, 10°, and 20° curves, respectively. If one assumes that the intensity of this peak has the functional form $I = I_0 \cos^2\theta + I_\pi \sin^2\theta$ for the p -polarization geometry, where I_σ and I_π are associated with σ - and π -like final states, respectively, and cross terms are omitted, then it is straightforward to estimate the ratio I_σ/I_π from the corrected peak heights. We find that I_σ/I_π (at $\hbar\omega = 192.0$ eV) is 0.05 ± 0.02 . By measuring the intensities in the range $194 \leq \hbar\omega \leq 195$ eV (relative to the tail of the Lorentzian fit to the $n = 1$ exciton), one finds that the ratio I_σ/I_π (in the $n > 1$ bound state and continuum region) is 0.05 ± 0.01 .

V. CONCLUSION

In this paper we have presented measurements of the optical absorption spectrum of hexagonal BN in the vicinity of the boron K threshold. The prominent peak in absorption at 192.0 eV varies with angle in the p -polarization geometry, indicating a mainly π -like final-state wave function. This is in agreement with both energy-loss experiments⁷ and the recent results of Barth *et al.*²² However, the experimental results are inconsistent with the final exciton state being constructed entirely of π -like wave functions. We suggest that the peak is due to an exciton state constructed mostly of π -like wave functions, with an admixture of σ -like wave func-

tions. By using a modified form of the effective-mass approximation, we estimate that the binding energy of the $n = 1$ core exciton state is 1.9 ± 0.2 eV.

The existence of an exciton state which displays σ - π mixing is plausible when one considers the band structures calculated using the OPW method. Tegeler *et al.*¹² find that OPW band calculations are in better agreement with x-ray emission experiments than tight-binding calculations. Moreover, the OPW calculations result in less separation of σ and π conduction bands, and hence greater σ - π mixing at a general point in the Brillouin zone. The extent of the $n = 1$ exciton state in \vec{k} space would result in the inclusion of σ wave functions in the expansion of the exciton state. There may be additional contributions due to higher-energy bands having σ -like symmetry.

The angular dependence of $n > 1$ exciton states is also consistent with σ - π mixing, and hence we conclude that the conduction band minimum may not be at a symmetry point (K or H) in the Brillouin zone. We estimate that the contribution in intensity due to the σ -like admixture is approximately 5%.

ACKNOWLEDGMENTS

The authors at the University of Illinois would like to acknowledge the support of the National Science Foundation under Grants Nos. DMR-79-13103 and 77-23999. The Synchrotron Radiation Center is supported by NSF Grant No. DMR-77-21888. The work of one of the authors (C.G.O.) is supported by U. S. DOE Contract W-7405-ENG-82, Office of Basic Energy Sciences, Division of Materials Science (AK-01-02).

*Present address: Department of Physics, University of Texas, Austin, TX 78712.

†Permanent address: Scuola Normale Superiore, 56100 Pisa, Italy.

¹J. Zupan and D. Kolar, *J. Phys. C* **5**, 3097 (1972).

²F. C. Brown, R. Z. Bachrach, and M. Skibowski, *Phys. Rev. B* **13**, 2633 (1976).

³V. A. Fomichev and M. A. Rumsh, *J. Phys. Chem. Solids* **29**, 2025 (1968).

⁴V. A. Fomichev, *Fiz. Tverd. Tela (Leningrad)* **9**, 3167 (1967) [*Sov. Phys.—Solid State* **9**, 2496 (1968)].

⁵W. Hayes and F. C. Brown, *J. Phys. B* **4**, L85 (1971).

⁶E. Doni and G. Pastori Parravicini, *Nuovo Cimento B* **64**, 117 (1969).

⁷R. D. Leapman and J. Silcox, *Phys. Rev. Lett.* **42**, 1361 (1979).

⁸F. C. Brown, R. Z. Bachrach, and N. Lien, *Nucl. Instrum. Methods*, **152**, 73 (1978).

⁹M. Altarelli and D. L. Dexter, *Phys. Rev. Lett.* **29**, 1100 (1972).

¹⁰R. Geick, C. H. Perry, and G. Rupprecht, *Phys. Rev.* **146**, 543 (1966).

¹¹W. Czaja, *Phys. Kondens. Mater.* **12**, 226 (1971).

¹²E. Tegeler, N. Kosuch, G. Wiech, and A. Faessler, *Phys. Status Solidi B* **91**, 223 (1979).

¹³B. Gerlach and J. Pollman, *Nuovo Cimento B* **38**, 423 (1977).

¹⁴A. Quattropani, F. Bassani, G. Margaritondo, and G.

- Tinivella, *Nuovo Cimento B* 51, 335 (1979).
- ¹⁵R. Resta, *Phys. Rev. B* 16, 2717 (1977).
- ¹⁶F. J. Rogers, H. C. Graboske, Jr., and D. J. Harwood, *Phys. Rev. A* 1, 1577 (1970).
- ¹⁷A. P. French and E. F. Taylor, *An Introduction to Quantum Physics* (Norton, New York, 1978), Secs. 4-5 and 5-8.
- ¹⁸J. Zupan *Phys. Rev. B* 6, 2477 (1972).
- ¹⁹A. Zunger, A. Katzir, and A. Halperin, *Phys. Rev. B* 13, 5560 (1976).
- ²⁰M. S. Nakhmanson and V. P. Smirnov, *Fiz. Tverd. Tela (Leningrad)* 13, 905 (1971); [*Sov. Phys.—Solid State* 13, 752 (1971)]; 13, 3288 (1971) [13, 2763, (1971)].
- ²¹M. Altarelli and W. Y. Hsu, *Phys. Rev. Lett.* 43, 1346 (1979); L. Resca and R. Resta, *Solid State Commun.* 29, 375 (1979); *Phys. Rev. Lett.* 44, 1340 (1980).
- ²²J. Barth, C. Kunz, and T. M. Zimkina, *Solid State Commun.* 36, 453 (1980).